Journal of Colloid and Interface Science 350 (2010) 110–116

Contents lists available at ScienceDirect

Journal of Colloid and Interface Science

www.elsevier.com/locate/jcis

Self-assembled monolayers of silver nanoparticles firmly grafted on glass surfaces: Low Ag^+ release for an efficient antibacterial activity

Piersandro Pallavicini [a,*], Angelo Taglietti [a,**], Giacomo Dacarro [a], Yuri Antonio Diaz-Fernandez [a], Matteo Galli [c], Pietro Grisoli [b], Maddalena Patrini [c], Giorgio Santucci De Magistris [a], Robertino Zanoni [d]

[a] Laboratorio di Nanochimica, Dipartimento di Chimica Generale, Università di Pavia, viale Taramelli 12 – 27100 Pavia, Italy
[b] Dipartimento di Farmacologia Sperimentale e Applicata, Università di Pavia, viale Taramelli 14 – 27100 Pavia, Italy
[c] Dipartimento di Fisica "A. Volta", Università di Pavia, via Bassi 6 – 27100 Pavia, Italy
[d] Dipartimento di Chimica, Università La Sapienza, piazzale Aldo Moro 5 – 00185 Roma, Italy

ARTICLE INFO

Article history:
Received 1 April 2010
Accepted 9 June 2010
Available online 15 June 2010

Keywords:
Antibacterial surface
Silver nanoparticles
Self-assembled monolayer

ABSTRACT

A two-step, easy synthetic strategy in solution has been optimized to prepare authentic monolayers of silver nanoparticles (NP) on MPTS-modified glass surfaces, that were investigated by AFM imaging and by quantitative silver determination techniques. NP in the monolayers remain firmly grafted (i.e. not released) when the surfaces are exposed to air, water or in the physiological conditions mimicked by phosphate saline buffer, as UV–Vis spectroscopy and AFM studies demonstrate. About 15% silver release as Ag^+ ions has been found after 15 days when the surfaces are exposed to water. The released silver cations are responsible of an efficient local microbicidal activity against *Escherichia coli* and *Staphylococcus aureus* bacterial strains.

1. Introduction

Bacterial infections involving the surface of medical devices (e.g. catheters, artificial prosthetics and subcutaneous implants) and more generally infections spread by materials used in the nosocomial environment are a serious challenge for bio-medical scientists [1]. In the last few decades a considerable effort was made to obtain antibacterial coatings on different surfaces, such as garments and medical devices [2]. The use of silver nanoparticles (NP) as antibacterial agents has been one of the most studied nanotechnology issues in the last decade [3]. Even if the debate concerning the true mechanism of their antibacterial action is still ongoing, it is generally accepted that it should involve Ag^+ release and its interaction with bacteria. Many applicative studies have been published [4]. The "layer-by-layer" (LbL) approach [5] has been applied to obtain surfaces on which thin films of silver NP are deposited or formed in situ on a molecular self-assembled monolayer (SAM) capable of interaction with silver [6]. In some cases the antibacterial activity of such surfaces has been evidenced [4d,7]. On the other hand, the increase of nanoparticle applications has raised the concern for health and environment risks connected to exposition and use of nanoparticles [8]. Nevertheless, with few exceptions [4f] NP layers appear to be weakly bound to the surface, with a consistent risk of NP release in the environment of application, that in perspective may be a human body. These considerations prompted us to find an efficient strategy to prepare glass surfaces with a monolayer of silver NP firmly grafted on a suitable molecular SAM. Our goal is to keep them confined to the surface and capable of exerting an efficient antibacterial activity thanks to Ag^+ release. Noticeably, this activity should be promoted by the high surface/mass ratio typical of NP. In addition, in an applicative perspective, preparing a monolayer of NP on a flat surface, instead of a film or a NP-loaded nanoporous matrix, reduces the amount of an expensive material used (silver) and intrinsically reduces the quantity of potentially dimension-risky materials (nano-objects) contained in the device.

We adopted a two-step process typical of the LbL approach, resembling that already successfully used for the preparation of a silver NP monolayer [9]. First, a SAM of a mercaptosilane is formed on activated glass, according to a procedure that has been optimized in our laboratories [10]. Then, the –SH terminated glass is immersed in a silver nanoparticles colloidal solution. This leads to the self-assembly of a NP monolayer covalently attached to the modified glass, as sketched in Scheme 1 [9b].

The two-step wet synthetic strategy has been optimized, obtaining a reliable protocol to prepare monolayers of silver NP on glass surface. The stability of the obtained NP monolayers under various conditions (including Phosphate Buffered Saline (PBS), mimicking physiological conditions) has been verified with UV-Vis spectroscopy, Atomic Force Microscopy (AFM) and X-ray

* Corresponding author. Fax: +39 0382 528544.
** Corresponding author. Fax: +39 0382 528544.
E-mail address: piersandro.pallavicini@unipv.it (P. Pallavicini).

0021-9797/$ - see front matter © 2010 Elsevier Inc. All rights reserved.
doi:10.1016/j.jcis.2010.06.019

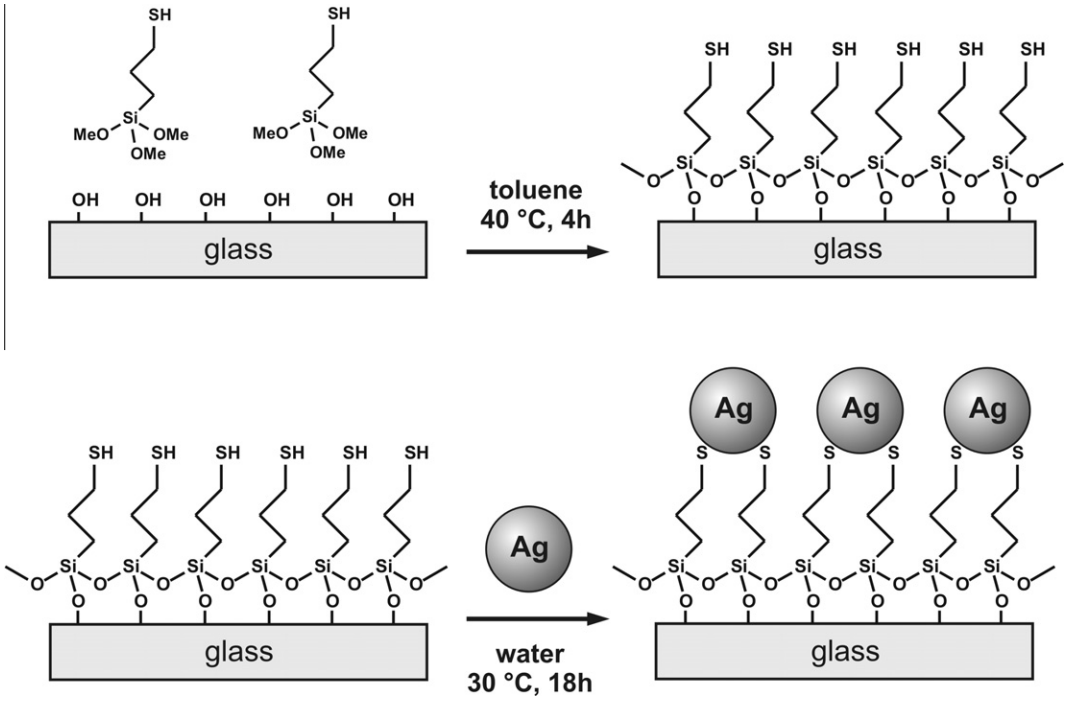

Scheme 1. Pictorial representation of the synthetic "layer-by-layer" approach used to prepare SAM of silver NP on glass substrates.

Photoelectron Spectroscopy (XPS). Ag^+ release and the consumption of the Ag NP monolayer have also been studied by means of inductively coupled plasma atomic emission spectroscopy (ICP-OES) and compared with the total Ag grafted on the surface. The antibacterial activity of the prepared glasses was investigated, finding an efficient microbicidal effect.

2. Material and methods

2.1. Materials

Silver nitrate (>99.8%), sodium borohydride (⩾99.0%), sodium citrate (>99.0%), (3-mercaptopropyl)trimethoxysilane (>97%, MPTS) and PBS were purchased from Sigma–Aldrich. Reagents were used as received. Microscopy cover glass slides (2.4 × 2.4 cm) were purchased from Forlab (Carlo Erba). Glass cuvettes were standard optical glass cuvettes purchased from Hellma. Water was deionized and then bidistilled.

2.2. Nanoparticle preparation

The synthesis of silver nanoparticles was adapted from a previously reported preparation [9a], see Supplementary data for experimental details. Dimensions (Transmission Electron Microscopy (TEM) images, see Supplementary data) were 7 nm (σ = 4 nm).

2.3. Preparation of a (3-mercaptopropyl)trimethoxysilane SAM on glass surface

The procedure is adapted from Ref. [10], see Supplementary data for full details.

2.4. Silver nanoparticle monolayer preparation

Thiol-modified glasses were immersed into the colloidal suspension of silver nanoparticles and kept at 30 °C for 18 h. In a typical preparation, eight glass slides were prepared at the same time, i.e. they were made to react in the same Ag NP suspension solution, inside a 8-place glass slides holder (where the slides were kept in a vertical position), placed in a large water bath thermostatted with a Julabo heating circulator, gently shaken on a Heidolph Promax 1020 reciprocating platform shaker. After this, the obtained yellow glasses were placed in water and sonicated for 5 min. This procedure was repeated twice, then the glasses were dried under a nitrogen stream and stored in air. The same procedure was applied to –SH terminated modified standard glass cuvettes.

2.5. Characterization

Absorbance spectra of colloidal suspensions were taken with a Varian Cary 100 spectrophotometer in the 200–1000 nm range. Spectra of NP-functionalized glasses were obtained placing the glasses on the same apparatus equipped with a dedicated Varian solid sample holder, or directly using the modified cuvettes. Measurements of absorbance vs. time on modified cuvettes were carried out by filling the cuvette with the chosen solution and keeping it stoppered and in the dark between successive spectra. For the determination of the local refractive index as a function of the solvent refractive index, a step-decreasing gradient of solvent polarity was followed in order to achieve the total removal of the previous solvent, i.e. the solvent was discarded, the cuvette was gently dried in a nitrogen flux and then washed three times with the next solvent before refilling. The following sequence of solvents was used: water, acetonitrile, DMF, *n*-butanol, ethyl acetate, toluene, *n*-heptane.

TEM images were obtained on colloidal solutions of Ag NP prepared as described in Section 2.2 and diluted ten times with bidistilled water, deposited on Nickel grids (300 mesh) covered with a Parlodion membrane and observed with a Jeol JEM-1200 EX II instrument.

Atomic force microscope images were obtained with a Thermo Microscopes CPII AFM, operated in tapping mode with NT-MDT silicon tips NSC05_10° and NSG01. Data analysis (manual width and height calculation on line profiles) was carried out with Image Processing and Data Analysis software – version 2.1.15 by TM Microscopes.

The total Ag content on glasses with NP monolayers was determined by quantitatively oxidizing the silver NP grafted on a single slide (24 × 24 mm or 12 × 24 mm) by dipping it in 5 ml ultrapure concentrated HNO_3 diluted 1:5 with water (13%w as final concentration) in a vial, and keeping it overnight at RT on a Heidolph Promax 1020 reciprocating platform shaker. The Ag content in solution was then determined by inductively coupled plasma (ICP) atomic emission spectroscopy. Release of Ag^+ vs. time was followed on a set of six Ag NP-coated glass slides (2.1 × 2.6 cm coated on both sides, total coated surface = 10.92 cm^2) prepared as described above. Each slide was then immersed in 3 ml of water. Slides were taken off the water at time = 5, 24, 48, 96, 288 and 456 h, the content of Ag^+ in the 3 ml water volume was determined by ICP-OES and the data expressed as the ratio of Ag μg to the surface from which they were released (ppm Ag × 3 ml/10.92 cm^2).

ICP-OES data were collected with an ICP-OES OPTIMA 3000 Perkin Elmer instrument.

XPS experiments were carried out on 1.0 × 1.4 cm quartz slides, with an experimental apparatus in UHV consisting of a modified Omicron NanoTechnology MXPS system, with an XPS chamber equipped with a dual X-ray anode source (Omicron DAR 400) and an Omicron EA-127 energy analyzer, and an attached VT-atomic force and scanning tunneling microscope (see Supplementary data for full details).

2.6. Antibacterial activity tests

The antibacterial activity of silver NP monolayers was investigated against *Staphylococcus aureus* ATCC 6538 (Gram+) and *Escherichia coli* ATCC 10,356 (Gram−). The microorganisms were grown overnight in Tryptone Soya Broth (Oxoid; Basingstoke, Hampshire, England) at 37 °C. Washed cells were resuspended in *Dulbecco's PBS* and optical density (OD) was adjusted to 0.1, at 600 nm wavelength corresponding approximately to 1×10^8 Colony Forming Units (CFU/ml).

Bacterial suspension (10 μl) was deposited on a standard microscope slide (76 × 26 mm); subsequently the microbial suspension was covered with a modified cover glass (24 × 24 mm), forming a thin film between the slides that facilitates direct contact of the microorganisms with the active NP surface. The two assembled glasses were introduced in a Falcon test-tube (50 ml) containing 1 ml of PBS to maintain a damp environment. For each bacterial strain two equivalent modified glasses were prepared; the slides were maintained in contact with the liquid films containing bacteria at room temperature for 5 and 24 h, respectively; for each time of contact an unmodified glass slide was treated the same way, giving a control sample. After the times of contact, 9 ml of PBS were introduced in each Falcon test-tube under a gentle shaking to detach the assembled glass slides. Bacterial suspensions were then grown in Tryptone Soya Agar (Oxoid; Basingstoke, Hampshire, England) to count viable cells.

The decimal-log reduction rate, microbicidal effect (ME), was calculated using the formula: $ME = \log N_C - \log N_E$ (N_C being the number of CFU/ml developed on the unmodified control glasses, and N_E being the number of CFU/ml counted after exposure to modified glasses). The results expressed as ME represent the average of three equivalent determinations.

3. Results and discussion

3.1. Nanoparticles preparation

Silver NP display the Localized Surface Plasmon Resonance (LSPR) [11] band, observed in absorption spectroscopy both for colloidal suspensions and for nanoparticles monolayers [12]. The intensity, the shape and the position of the LSPR bands depend on the size and shape of the nanoparticles [13], on the stabilizing agents covering the NP surface, and on the dielectric constant of the surrounding environment [12a]. In the case of spherical silver nanoparticles with size <50 nm of diameter, this band is around 400 nm [12a].

In our preparations, the spectra of citrate-stabilized silver NP showed an LSPR peak centered at λ = 394 nm in aqueous solutions. Several preparations were repeated, giving reproducible results (see Supplementary data, Fig. S1). This synthetic procedure yielded spherical NP with a large size distribution, i.e. ~7 ± 4 nm diameter (TEM images, Supplementary data, Fig. S2a–d) colloidal solutions were stored without particular care in glass flasks, and stability of NP was monitored recording several spectra during 4 weeks, showing no detectable changes of the LSPR peak.

3.2. Silver NP SAM

Spectra of silver nanoparticles grafted on MPTS-modified glass slides were measured in air, after drying the slides with a nitrogen stream. In this case the LSPR peak was found to be at the average λ_{max} = 390 nm (σ = 4 nm). However, as it can be seen in Fig. 1a, the background absorbance is very intense and may significantly affect also the read peak position (λ_{max}). Accordingly, the absorbance spectra were analyzed using a home-made software, that allows the background to be interpolated with a cubic-spline and subtracted from the experimental curves, as already reported in the literature [10]. As an example, Fig. 1b shows the spectra of Fig. 1a after normalization. From the normalized spectra the parameters of the peaks can be accurately determined (λ_{max} and its FWHM, full width at half maximum). All the values mentioned and used in this work will be taken from normalized spectra unless otherwise stated. The maximum absorbance for corrected spectra of Ag nanoparticles monolayers on glass slides occurs at λ_{max} = 398 nm. This value is the average on five preparations (33 slides on a total of 40; seven slides were discarded, vide infra), with a standard deviation of 4 nm only. Although we obtained reproducible λ_{max} values (peak lineshape was not changing too), we observed significantly different absorbance intensities, so we adopted this selection procedure: (i) in a typical synthesis eight glass slides were prepared simultaneously from the same freshly prepared silver NP solution; (ii) a spectrum was recorded for each NP-covered glass slide of the same 8-piece preparation, measuring the absorbance intensity A_{398} at the LSPR peak; (iii) the average

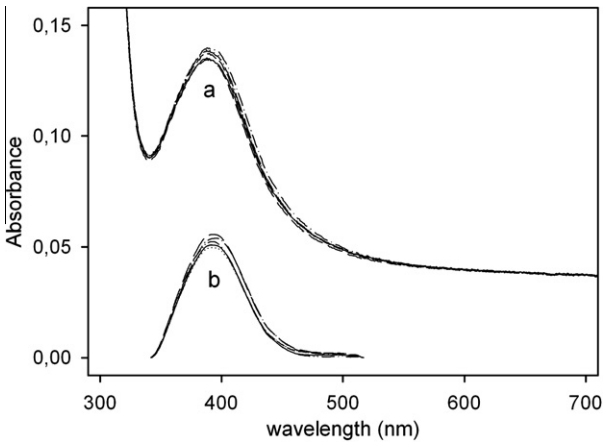

Fig. 1. Spectra of a set of six modified glasses obtained in a single preparation: (a) uncorrected and (b) after background subtraction (only the 350–520 nm interval is shown. Due to the numerical subtraction method for λ < 350 nm and λ > 520 nm the calculated absorbance is 0).

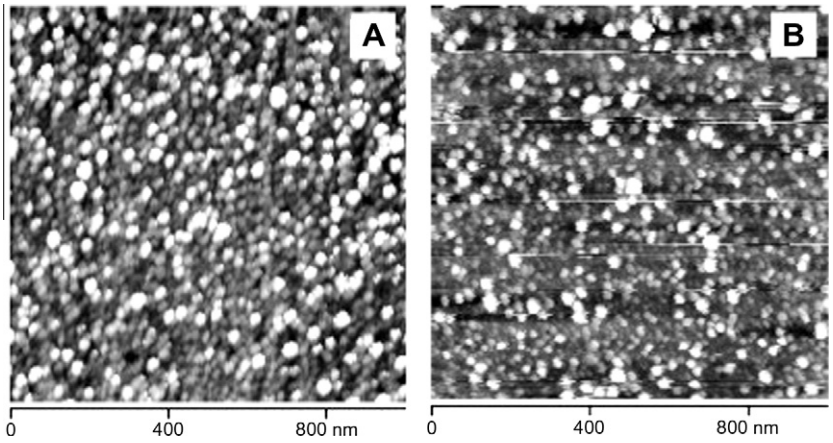

Fig. 2. (A) AFM image on a freshly prepared glass slide covered with silver NP and (B) AFM image of the same glass slide kept in bidistilled water for 19 days.

absorbance peak value was calculated and only the samples with an absorbance whose difference to the average value was within the standard deviation were used, while the others were discarded. On five 8-piece preparations, 33 slides on 40 (82%) were kept. Fig. 1 reports the spectra recorded for a set of six glass slides obtained from a 8-piece preparation, with absorbance falling near to the average value.

Silver NP-modified glass slides are stable in air, i.e. their spectra do not change significantly in a 2 weeks period. Atomic Force Microscopy images were taken on a freshly prepared NP-modified glass, after drying, see Fig. 2A (see also Supplementary data, Fig. S3, for AFM images taken on air-exposed slides after 2 weeks). Although average dimensions and polydispersity cannot be directly calculated using a dedicated software (due to the high density of objects), on these AFM images the dimensions of NP on the surface appear larger than those observed in the parent colloidal solution. The analysis of line profiles on 250×250 nm and 500×500 nm images yielded a statistic value of the average diameter of 25 ± 6 nm (Table S1, Supplementary data). However, the dimension increase is only apparent. In tapping-mode AFM convolution of the finite tip size (10 nm curvature radius in our case) with true surface morphology is known to result in overestimated in-plane dimensions of an object, if its width is comparable with the tip curvature (apparent >3× real dimensions) [14]. An empirical calculation relating the tip curvature radius, the object radius and the visualized width of the imaged object [15] when applied to our case, i.e. tip curvature radius = 10 nm and NP radius = 3.5 nm, would result in an observed width of 25 nm. On the other hand, as expected [14,15], the measurement of average particle height from line profile analysis gives an average value $h = 5.6$ nm (±1.9 nm) that is consistent with the diameter value determined by TEM.

We completed the characterization of the grafted NP monolayer by means of quantitative oxidation of the silver NP and analysis of the obtained Ag^+ solution by means of ICP-OES (see experimental for details). From 14 experiments we found an average of 3.57×10^{-7} g/cm^2 ($\sigma = 7.2 \times 10^{-8}$) of silver. Considering silver NP of 7 nm in diameter (volume = 179.503 nm^3, mass = 1.88299×10^{-18} g, using $d_{Ag} = 10.49$ g/cm^3), such a surface concentration would correspond to 118 NP in an area of 250×250 nm, nicely fitting with the 127 NP counted on AFM images (Fig. S4, Supplementary data).

ICP-OES data coupled with the observation of AFM images, strongly indicate that a *single* layer of silver nanoparticles is obtained on our modified glass surfaces. It has to be noted that the literature mentions the possibility of observing significant shifts and changes in the shape of LSPR peaks when noble metal nanoparticles are placed in 2D arrays at distances shorter than the particles dimension [9a,12a,16]. In our case we observed only a 4 nm shift from colloidal solution to the NP-functionalized glass surface in air, with no significant change in the peak FWHM (see also Fig. S1b, Supplementary data). Moreover, this small shift should as well be attributed to the change in the layer covering the NP [12a] and in the dielectric constant around them [12a], dictated by the replacement of a significant part of the stabilizing citrate anions by thiolate on the portion of each NP surface grafted on glass, and by the removal of citrate from the remaining, not glass-facing part of the NP surface, reasonably with the formation of a thin oxide layer (vide infra). According to the literature [16a,16b], the ratio $D/2r$ affects both the LSPR position and its lineshape, with D = distance between adjacent particles centers and $2r$ = diameter of the particles. Although AFM images clearly show an irregular disposition of the silver NP (see also Fig. S5, Supplementary data), a rough evaluation of the average interparticle distance can be made placing the ~120 NP found in the 250×250 nm image in a cubic two dimensional arrangement, obtaining $D = 24$ nm and $D/2r = 3.4$. At this $D/2r$ value, the position of the LSPR peak is only few nanometers shifted and its lineshape indistinguishable from those of an isolate particle [16a,16b], in agreement with our λ_{max} and FWHM data.

According to Scheme 1 and in agreement with AFM images, part of the NP surface remains exposed to the environment and part is hindered by the thiol-mediated contact with glass. We studied the influence of the dielectric constant of the environment by recording the absorbance spectra on the NP-functionalized walls of standard glass cuvettes, first in water and then in a series of solvents (acetonitrile, dimethylformamide, *n*-butanol, toluene, *n*-heptane, ethyl acetate). The normalized spectra were interpreted applying the Mie's formalism [17] combined with the dielectric function data for silver [18]. This approach allows us to calculate the effective refractive index (n_{eff}) felt by the NPs anchored to the thiol-functionalized surface when exposed to different solvents (see ESI for details). The results are shown in Fig. 3, and display a sharp correlation of n_{eff}^2 with the squares of the refractive index of the medium [19]. Noticeably, the LSPR absorbance peak of a NP monolayer grafted on cuvette walls first dried and then filled with water is 413 nm (average value, $\sigma = 3$ nm),[1] with respect to the 394 nm

[1] When NP monolayers are prepared on cuvette walls, spectra measured on dried surfaces display a more scattered series of λ_{max} values, distributed in the range 396–408 nm. However, all cuvettes, when filled in water, change λ_{max} sharply to the same value (413 nm). This suggests that the LSPR absorption position depends on the degree of absorbed humidity on the examined surface and that the drying procedure is obviously less straightforward when carried out in a, almost closed, tiny container as a spectroscopy cuvette.

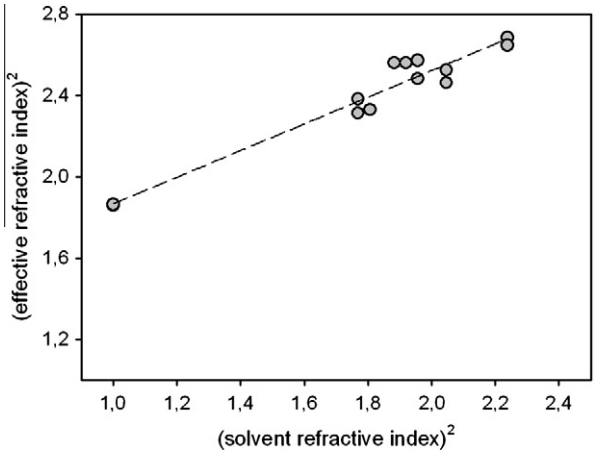

Fig. 3. Gray circles: squares of effective refractive index felt by NP (calculated from absorbance spectra of NP surface dipped in the chosen solvent) coupled with the squares of tabulated refractive index of the chosen solvent (two series of measurements are reported); dashed line: linear fit ($r^2 = 0.95$). The points refer to the following solvents: no solvent (air, $n_d = 1$), water (1.3330), acetonitrile (1.3442), ethyl acetate (1.3723), *n*-heptane (1.3855), *n*-butanol (1.3988), dmf (1.4305), toluene (1.4961).

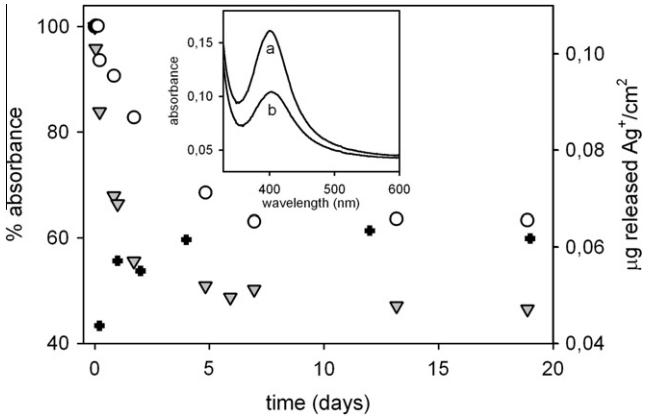

Fig. 4. Percent absorbance (with respect to the initial value) vs. time on cuvettes with walls modified with a silver NP monolayer when filled with bidistilled water (gray triangles) or Phosphate Buffered Saline solution (white circles), left vertical axis. Black crosses: μg of released Ag^+/cm^2 of exposed surface vs. time (each point is an average of three values), right vertical axis. Inset: absorbance spectrum, on a modified cuvette filled with bidistilled water: (a) spectrum recorded at $t = 0$ and (b) same at $t = 19$ d (uncorrected spectra).

value of the citrate-capped monodisperse colloidal NP, and to the 398 nm found for dry glass slides.

The linear fit of n_{eff} vs. the medium refractive index (Fig. 3 dashed line) is good ($r^2 = 0.95$), and from the slope of the fitting line it is possible to evaluate the fraction of silver NP surface exposed to the solvent (see Supplementary data for calculation details). We calculated that 66% of the NP surface is directly exposed to the solvent. Accordingly, the position and shape of the observed spectra are influenced by a combination of the contributions of the interaction of the thiol units on the side of the NP facing the glass surface and of the external environment on the exposed side.

3.3. Stability of the NP SAM and Ag^+ release

In order to establish the behavior of silver NP monolayers when exposed to water as a function of time we used standard glass cuvettes functionalized on the internal walls with NP and examined both the spectroscopic behavior of the monolayers and the amount of released Ag^+. The cuvettes were filled with bidistilled water, capped with a Teflon stopper and stored at RT for a period of 19 days. During this time, UV–Vis spectra were taken at 12–24 h intervals.

While the position of the LSPR peak remained unchanged, a significant variation in intensity was observed. Fig. 4, gray triangles, reports the variation of the absorbance value at 413 nm with time (expressed as percentage of the initial absorbance). The peak intensity decreases reaching a plateau after 3 days. A shift of 3 nm towards longer wavelengths is also observed for λ_{max}. Fig. 3, inset, shows the spectra recorded a $t = 0$ (a) and at $t = 19$ days (b).

The absorbance decrease has no straightforward explanations. It has been already stressed that NP shape and dimensions may affect the features of LSPR peaks [12a,16], and of course the absorbance intensity is expected to be proportional to the quantity of grafted NP on the glass surface. However, significant consumption of Ag NP or their detachment from the glass surface can be ruled out: at the end of the 19 days measurements period, the 3 ml water samples contained in the cuvette were analyzed through ICP-OES to evaluate the total content in silver, which was found to be 0.23 ppm, corresponding to a total of 0.69 μg of metal released from glass. On the basis of our ICP-OES data on freshly prepared glasses, and assuming the cuvette surface covered with nanoparticles to be 13 cm^2, a starting total amount of 4.64 μg of silver on the cuvette walls was calculated. This means that only 15% of the silver originally deposed on glass via SAM formation was released in water during 19 days. Moreover, the spectra of the water solution exposed to NP-modified cuvette did not show any LSPR absorbance after the 19 d period. These observations well fit to the AFM images obtained on silver NP-functionalized glass slides kept in bidistilled water for the same time, under the same conditions (Fig. 2b). The AFM images show NP layers approximately identical to those obtained for a modified glass before immersion in water (Fig. 2a), both in the morphological and dimensional features of the surface-grafted NP. The quantity of released Ag^+ vs. time was also measured with an independent experiment on a set of six glass slides (see experimental). The obtained data, expressed as μg of released Ag^+/cm^2 of exposed surface (Fig. 4, black crosses) show a trend comparable to that of the absorbance vs. time evolution.

Adsorption of electrolytes on NP surface is known to affect LSPR features [20], but it is obviously ruled out in the experiments in cuvette with bidistilled water. However, it has been reported that also the oxidation of metal atoms on the NP surface influences the LSPR features [21]. In our opinion, it is the formation or the thickening of a Ag_2O layer on the water-exposed surface of silver NP the responsible of the observed time evolution of LSPR peaks, with the formation of an oxidized silver layer in the initial 3-days period, reaching a steady-state in which the slowly released Ag^+ ions are replaced by Ag oxidized from the bulk. To further investigate this, XPS experiments have been carried out on quartz slides modified with an Ag NP monolayer, after being aged in air and in water for 1 week. Assignment to Ag and Ag oxides of the XPS lines was performed by taking into account both the direct photoemission line Ag 3d and the auger line MNN. For the sample aged in water the only detected silver signal corresponds to Ag_2O, while in the case of the air-exposed sample both elemental Ag and Ag_2O are detected. Significantly, as a value of 1.3 nm was reported for the inelastic mean free path of Ag 3d photoelectrons excited by Mg Kα photons [22], the overall oxide layer should not exceed that value for the sample aged in air, while it is significantly thicker in the case of water-aged sample (see Supplementary material for a detailed discussion and XPS spectra).

Table 1
Microbicidal effect (ME) of silver NP-modified glass after 5 and 24 h of contact.[a]

	Contact time	
	5 h	24 h
Bacterial strain	ME	
S. aureus ATCC 6538	1.37	5.54
E. coli ATCC 10356	4.93	5.90

[a] Reported data are the average of three experiments.

The evolution of the silver NP monolayer was also observed on functionalized cuvettes exposed to Phosphate Buffered Saline (PBS). Absorbance vs. time profiles and the small λ_{max} red shift were similar to what found with water, see Fig. 4, white circles.[2]

3.4. Antibacterial activity tests

Table 1 shows the results of the evaluation of microbicidal effect (ME) [23] of the modified glass slides. In order to understand if a surface modified with our silver NP monolayer would be efficient in preventing the development of local infections, we need to evaluate the microbicidal effect exerted on physiological fluids in contact with the surface. Moreover, also considering the small amount of silver released from functionalized glass surfaces, antibacterial activity could not be evaluated through classical methods, such as the measure of inhibition halos on agar plates or the determination of the minimum inhibitory concentration (MIC) in nutrient broth. We developed a practical test that simulates real-life conditions of use for our modified glasses and allows the evaluation of the bactericidal effect in a thin liquid film in contact with the surface. Details about the method are described in the relevant section of experimental. *S. aureus* and *E. coli* were used as commonly considered representative strains for the evaluation of antibacterial activity of drugs [4]. ME is remarkable after 24 h of contact on both the bacterial strains used. *S. aureus* seems to be less sensitive after 5 h of contact and this result is in agreement with the observed lowered efficiency of silver NPs on gram-positive strain [4c] (although the result reported in Ref. [4g] is obtained with monodispersed NP colloidal solutions). Remarkably, in the tests proposed by EN 13697 [24] the microbicidal activity of a disinfectant is considered acceptable when the decimal-log reduction rate (i.e. ME), is at least equal to 4 after 5 min of contact. In our case ME of the modified glass is superior to 4 even after 5 h of contact for *E. coli*, while for *S. aureus* ME overcomes 4 after 24 h.

The results clearly indicate an efficient and long-lasting local microbicidal effect exerted by the NP-modified glass surfaces. As surface characterization of the NP-covered slides has evidenced a non-compact monolayer of silver NP, with the presence of some unreacted –SH groups, control experiments were also carried out on glasses modified with the only MPTS monolayer, i.e. with no grafted Ag NP. In this case the ME was completely absent.

4. Conclusions

In this study a silver NP monolayer has been successfully immobilized on glass using the LbL technique, obtaining a satisfactory coverage of the surface (3.57×10^{-7} g of Ag per cm^2, corresponding to $\sim$1900 NP/μm^2) and glass surfaces that are stable for weeks in dry conditions. While the NP surface facing glass is hindered by thiol interaction, the remaining surface (ca. 66%) is exposed to the environment and interacts with it. The behavior of the modified glass surfaces has been studied when exposed to water and PBS, finding that only $\sim$15% of the total quantity of silver loaded on the monolayer is released in solution, even after a 19 days period, probably by the oxidation of the medium-exposed part of the NP surface. Moreover, no detachment of NP from the surface has been observed. Nevertheless, a strong antibacterial activity was found, both towards gram-negative and gram-positive representative bacterial strains. A glass-like SiO_2 film can be easily deposited on a large spectrum of materials by gelification of a siloxane sol and the LbL procedure here described can be applied also in that case: we can thus envisage the use of our approach to produce materials displaying an intrinsic antibacterial effect, with negligible toxicity connected to Ag^+ release and with drastically reduced risk as regards in vivo contamination with objects of nanometric scale. Although these materials would be of poor use in flow-through or large volume systems (due to the small amount of released Ag^+), medical devices requiring a short, local action against the development of infections on their surface (e.g. catheters, artificial prosthetics and subcutaneous implants) could advantageously profit of the coating described here.

[2] PBS is a buffer solution commonly used in bio-medical research, as it is isotonic to cells and non toxic. It is 0.01 M in sodium hydrogenphosphate, 0.138 M in NaCl and 0.0027 M in KCl, with pH = 7.4. No LSPR bands were found in solution after 19 days exposure. In this medium, due to matrix effect, it was not possible to estimate via ICP measurements the Ag^+ concentration released in solution.

Acknowledgments

Authors acknowledge financial support by Fondazione Cariplo (Bandi Chiusi 2007, "Superfici vetrose a azione antimicrobica basata sul rilascio modulato e controllato di cationi metallici") and by Regione Lombardia (G. Dacarro Grant, Project REGLOM16). We gratefully thank Dr. Lucia Cucca (Dipartimento di Chimica Generale, Università di Pavia) for ICP-OES measurements, Dr. Vittorio Necchi (Centro Grandi Strumenti, Università di Pavia) for TEM images, and Dr. Massimo Tonelli (C.I.G.S. – Centro Interdipartimentale Grandi Strumenti, Università di Modena e Reggio Emilia) for additional AFM images. We also thank Dr. Jose Manuel Fernandez Echevarria (BIOINFO, Instituto Superior de Tecnologia y Ciencias Aplicadas, La Habana, Cuba – CICOPS visiting fellow at Università di Pavia) for the compilation of the spectra normalization software and for the fruitful discussion.

Appendix A. Supplementary material

Supplementary data associated with this article can be found, in the online version, at doi:10.1016/j.jcis.2010.06.019.

References

[1] E.M. Hetrick, M.H. Schoenfisch, Chem. Soc. Rev. 35 (2006) 780.
[2] (a) P.N. Danese, Chem. Biol. 9 (2002) 873;
(b) K. Lewis, A.M. Klibanov, Trends Biotechnol. 23 (2005) 343.
[3] (a) E. Weir, A. Lawlor, A. Whelan, F. Regan, Analyst 7 (2008) 835;
(b) M. Rai, A. Yadav, A. Gade, Biotechnol. Adv. 27 (2009) 76;
(c) E.J. Fernandez, J. Garcia-Barrasa, A. Laguna, J.M. Lopez-de-Luzuriaga, M. Monge, C. Torres, Nanotechnology 19 (2008) 185602;
(d) G.A. Martìnez-Castanon, N. Nino-Martìnez, F. Martìnez-Gutierrez, J.R. Martìnez-Mendoza, F. Ruiz, J. Nanoparticle Res. 10 (2008) 1343.
[4] (a) I. Sondi, B. Salopek-Sondi, J. Colloid Interface Sci. 275 (2004) 177;
(b) J. Kim, J. Ind. Eng. Chem 13 (2007) 718;
(c) S. Pal, Y.K. Tak, J.M. Song, Appl. Environ. Microbiol. 73 (2007) 1712;
(d) Z. Li, D. Lee, X. Sheng, R.E. Cohen, M.F. Rubner, Langmuir 22 (2006) 9820;
(e) Y. Zhang, H. Peng, W. Huang, Y. Zhou, D. Yan, J. Phys. Chem. C 112 (2008) 2330;
(f) K. Yliniemi, M. Vahvaselka, Y. Van Ingelgem, K. Baert, B.P. Wilson, H. Terryn, K. Kontturi, J. Mater. Chem. 18 (2008) 199;
(g) S. Shrivastava, T. Bera, A. Roy, G. Singh, P. Ramachandrarao, D. Dash, Nanotechnology 18 (2007) 225103.
[5] (a) L. Netzer, J. Savig, J. Am. Chem. Soc. 105 (1983) 674;
(b) H. Lee, L.J. Kepley, H.G. Hong, T.E. Mallouk, J. Am. Chem. Soc. 110 (1988) 618;
(c) H.C. Yang, K. Aoki, H.G. Hong, D.D. Sackett, M.F. Arendt, S.L. Yau, C.M. Bell, T.E. Mallouk, J. Am. Chem. Soc. 115 (1993) 11855.

[6] (a) R.F. Aroca, P.J.G. Goulet, D.S. dos Santos, R.A. Alvarez-Puebla, O.N. Oliveira, Anal. Chem. 77 (2005) 378;
(b) N.P.W. Peczonka, P.J.G. Goulet, R.F. Aroca, J. Am. Chem. Soc. 128 (2006) 12626;
(c) Q. Zhou, Q. Fan, Y. Zhuang, Y. Li, G. Zhao, J. Zheng, J. Phys. Chem. B 110 (2006) 12029;
(d) D. Pristinksi, S. Tan, M. Erol, H. Du, S. Sukhishvili, J. Raman Spectrosc. 37 (2006) 762.
[7] D. Lee, R.E. Cohen, M.F. Rubner, Langmuir 21 (2005) 9651.
[8] A.L. Neal, Ecotoxicology 17 (2008) 362.
[9] (a) R.M. Bright, M.D. Musick, M.J. Nathan, Langmuir 14 (1998) 5695;
(b) F. Frederix, J.M. Friedt, K.H. Choi, W. Laureyn, A. Campitelli, D. Mondelaers, G. Maes, G. Borghs, Anal. Chem. 75 (2003) 6894.
[10] (a) P. Pallavicini, G. Dacarro, M. Galli, M. Patrini, J. Colloid Interface Sci. 332 (2009) 432;
(b) S. Pan, Z. Wang, L.J. Rothberg, J. Phys. Chem. B 110 (2006) 17387.
[11] (a) C. Burda, X. Chen, R. Narayanan, M.A. El-Sayed, Chem. Rev. 105 (2005) 1025;
(b) Y. Xia, N.J. Halas, MRS Bull. 30 (2005) 338.
[12] (a) A. Moores, F. Goettmann, New J. Chem. 30 (2006) 112;
(b) D.D. Evanoff Jr., G. Chumanov, ChemPhysChem 6 (2005) 1221.
[13] B. Wiley, Y. Sun, Y. Xia, Acc. Chem. Res. 40 (2007) 1067.
[14] K.C. Grabar, K.R. Brown, C.D. Keating, S.J. Stranick, S.L. Tang, M.J. Natan, Anal. Chem. 69 (1997) 471.
[15] C. Bustamante, J. Vesenka, C.L. Tang, W. Rees, M. Guthold, R. Keller, Biochemistry 31 (1992) 22.
[16] (a) C.L. Haynes, A.D. McFarland, L.L. Zhao, R.P. Van Duyne, G.C. Schatz, L. Gunnarsson, J. Prikulis, B. Kasemo, M. Kall, J. Phys. Chem. B 107 (2003) 7337;
(b) L.L. Zhao, K.L. Kelly, G.C. Schatz, J. Phys. Chem. B 107 (2003) 7343;
(c) B.H. Choi, H.H. Lee, S. Jin, S. Chun, S.H. Kim, Nanotechnology 18 (2007) 075706.
[17] U. Kreibig, M. Vollmer, Optical Properties of Metal Clusters Springer Series in Materials Science, vol. 25, Springer-Verlag, Berlin Heidelberg, 1995.
[18] E.D. Palik, Handbook of Optical Constants of Solids, Academic Press, New York, 1985.
[19] Refractive indexes (source: CRC Handbook of Chemistry and Physics 87th edition, Taylor & Francis): water 1.3300; acetonitrile 1.3442; ethyl acetate 1.3723; *n*-heptane 1.3855; *n*-butanol 1.3988; dimethylformamide 1.4305; toluene 1.4961.
[20] T. Linnert, P. Mulvaney, A. Henglein, J. Phys. Chem. 97 (1993) 679.
[21] (a) C. Lok, C. Ho, R. Chen, Q. He, W. Yu, H. Sun, P.K. Tam, C. Che, J. Biol. Inorg. Chem. 12 (2007) 527;
(b) P. Mulvaney, T. Linnert, A. Henglein, J. Phys. Chem. 95 (1991) 7843.
[22] A. Jablonski, S. Tougaard, J. Vac. Sci. Technol., A 8 (1990) 106.
[23] A.D. Russel, W.B. Hugo, G.A.J. Ayliffe (Eds.), Principles and Practice of Disinfection, Preservation & Sterilization, Blackwell Publishing, 2004.
[24] CEN (CEN European Committee for Standardization) EN 13697 Chemical Disinfectants and Antiseptics – Quantitative Non-porous Surface Test for the Evaluation of Bactericidal and/or Fungicidal Activity of Chemical Disinfectants used in Food, Industrial, Domestic and Institutional Areas – Test Method and Requirements (Phase 2, Step 2), Brussells: CEN, 2002.